10th IMEKO TC14 Symposium on
Laser Metrology for Precision Measurement and Inspection in Industry
Braunschweig, GERMANY, 2011, September 12-14

In-Process Roundness Measurements of Steel Rings during Gas Quenching

Presentation and Assessment of the Optical Displacement Sensors

H. Gafsi, **G. Goch**, Bremen, Germany

Abstract:

This paper reports on the optical displacement sensors of a semi-optical system for measurements of roundness deviations of steel rings (~ 72.5 mm) during gas quenching. They are based on the extrinsic intensity modulation principle. The measurement system was developed within the scope of the Collaborative Research Centre SFB 570 of the German Research Foundation for investigation on the distortion of steel workpieces. Due to its capability for in-process measurements, this system also enables to compensate distortion effects. It is applied in a gas nozzle field specially designed for quenching steel rings symmetrically or asymmetrically with a broad variety of spatial temperature distributions. Before quenching, the ring has a starting temperature of 900 °C.

The measurement system has been built and successfully tested. It is able to measure the change of the roundness deviation of a hot ring during quenching. Before the calibration of the whole system, the sensors should be characterised and assessed.

Introduction

As a heat treatment process, gas quenching is one of the last steps in the industrial production process of steel component parts. This process often leads to undesired distortion, which has to be minimized by costly finishing treatments like grinding. In case of steel rings, the distortion mainly appears as roundness and wall thickness deviations.

The Collaborative Research Center ‘Distortion Engineering’ (SFB 570) of the German Research Foundation investigates the origin and the cause of distortion along the entire production chain with the goal to develop compensation strategies. Therefore, a gas nozzle field was specially designed with the ability to quench symmetrically or asymmetrically. So, it is possible to induce thermally generated ‘counter’ deformation to compensate existing roundness deviations of the distorted ring [1, 2, 3]. But, the knowledge about the roundness deviation is required for this compensation process. For this duty, a semi-optical and in-process measurement system is applied in the nozzle field.

Measurement setup and theory

The gas nozzle field consists of 12 outer and 12 inner gas nozzles, which are distributed along the ring circumference. A former publication describes the nozzle field in detail [4]. Between each two outer nozzles, one tactile and two non-contact optical sensors are placed. Thereby, only one of the optical sensors is active and the other acts as an additional light source to increase the measurement resolution. So, the measurement system consists effectively of 12 optical and 12 tactile displacement sensors. They act independently from each other and due to there number, they can deliver information about the ring mean radius (0^{th} Fourier order), the ring eccentricity (1^{st} Fourier order) and the roundness deviations from ovality (2^{nd} Fourier order) to pentagonality (5^{th} Fourier order). The tactile sensors can acquire in-situ the absolute geometrie information of the hot ring. But during the quenching, they cannot measure due to turbulence by the gas flow. At this point, the optical sensors resume the measurements.

The calibration of the tactile sensors was successful [5]. The routine bases on a model with nonlinear equations, which represents the trigonometric relationship between the raw measurement data and the CMM (coordinate measurement machine) measured form information (mean radius and roundness deviations) of several rings. To calibrate the optical sensors, this model requires the knowledge about the distance dependency of their raw data without disturbance by surface effects like roughness or reflectivity.

The measurement technique of the optical displacement sensors bases on the extrinsic intensity modulation [5, 6]. In principle, it employs a light source with a divergent radiation beam and two light detectors (or detector groups). The detectors have a conical and restricted acceptance angle and a different distance to the light source. Every detector acts with the light source as an independent sensor with a characteristic curve according to its modulation function M, which depends implicitly on the distance and is linear proportional to the reflectivity r of the surface in front of the sensor [7]. The quotient of the two modulation functions results in a reflectivity compensated characteristic curve depending on the distance only.

The sensors presented in this paper employ a green (532 nm) LED as the light source and 4 phototransistors as light detectors (Figure 1). A band-pass glass filter in front of the sensor minimizes the reception of interfering light like infrared radiation from the hot ring and ambient light. The phototransistors are in line with the LED in the middle and build two groups: the inner group (close to the LED) and the outer group (far from the LED). Each group acts with the same LED respectively as an inner or outer sensor element and delivers a voltage signal U_{PT}, which is linearly proportional to the detected emissive power Φ_{PT}:

$$\Phi_{PT} \rightarrow U_{PT} = U_{PT,offset} + \int_{\lambda} S_{PT}(\lambda) \cdot \Phi_{PT}(\lambda) \cdot d\lambda \,. \tag{1}$$

S_{PT} is the spectral sensitivity of the phototransistors and $U_{PT,offset}$ is the measured dark voltage. According to the super position principle, Φ_{PT} results from the reflection on the surface in front of the sensor, the internal reflection in the glass filter and the remaining interfering light Φ_{amb} getting through the glass filter additively:

$$\Phi_{PT}(\lambda) = (1 - r_{\text{int}}) \cdot M \cdot \Phi_{LED} + r_{\text{int}} \cdot \Phi_{LED} + \Phi_{amb} \tag{2}$$

with

$$M = f(X_{EIM}, r) = g(X_{EIM}) \cdot r \,. \tag{3}$$

The factor r_{int} represents the fraction of the LED emissive power Φ_{LED}, which is reflected within the glass filter. X_{EIM} is the distance between the surface and an arbitrarily defined virtual point of origin on the measurement direction of the sensor.

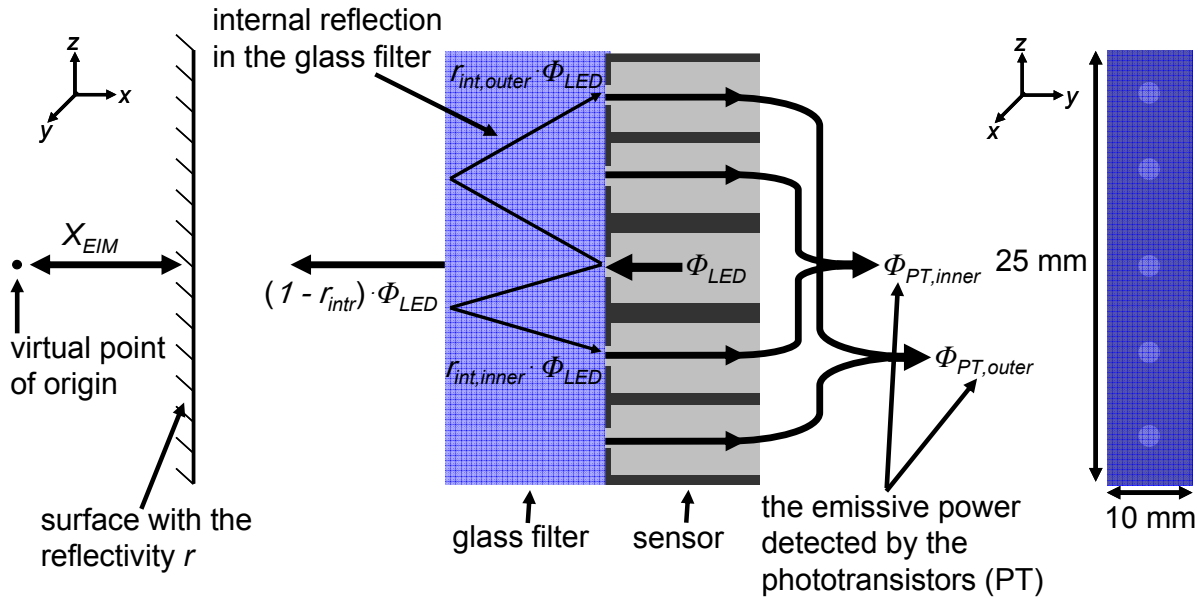

Fig. 1: Schematic views of the optical sensor.

The spectral distribution of the first two summands in equation (2) is restricted by the full width half maximum (FWHM) of the LED light. According to the data sheet of the phototransistors, S_{PT} can be assumed as a constant in this spectral range and will be considered as the factor $S_{PT,\lambda}$. After inserting equation (2) in equation (1), this fact leads to:

$$U_{PT} = U_{PT,offset} + S_{PT,\lambda} \cdot (1 - r_{\text{int}}) \cdot M \cdot \Phi_{LED} + S_{PT,\lambda} \cdot r_{\text{int}} \cdot \Phi_{LED} + \int_{\lambda} S_{PT}(\lambda) \cdot \Phi_{amb}(\lambda) \cdot d\lambda \,. \tag{4}$$

Here, the first and the last summand don't depend on Φ_{LED} and can therefore be filtered by pulsed operation of the LED (Lock-In-technique):

$$U_{PT} = S_{PT,\lambda} \cdot (1 - r_{\text{int}}) \cdot M \cdot \Phi_{LED} + S_{PT,\lambda} \cdot r_{\text{int}} \cdot \Phi_{LED} \,. \tag{5}$$

The modulation function for each of the two sensor elements can be expressed by the following equations:

$$M_{inner} = \frac{U_{PT,inner} - S_{PT,\lambda,inner} \cdot r_{\text{int},inner} \cdot \Phi_{LED}}{(1 - r_{\text{int},inner}) \cdot S_{PT,\lambda,inner} \cdot \Phi_{LED}} = \frac{U_{PT,inner} - k_{1,inner}}{k_{2,inner}} \tag{6}$$

and

$$M_{outer} = \frac{U_{PT,outer} - S_{PT,\lambda,outer} \cdot r_{\text{int},outer} \cdot \Phi_{LED}}{(1 - r_{\text{int},outer}) \cdot S_{PT,\lambda,outer} \cdot \Phi_{LED}} = \frac{U_{PT,outer} - k_{1,outer}}{k_{2,outer}} \,. \tag{7}$$

The k-terms are constants. The quotient of M_{outer} and M_{inner} leads to the reflectivity compensated modulation function M_q of the sensor:

$$M_q = k_2 \cdot \frac{U_{PT,outer} - k_{1,outer}}{U_{PT,inner} - k_{1,inner}} = k_2 \cdot Q_{EIM} \tag{8}$$

with

$$k_2 = \frac{k_{2,inner}}{k_{2,outer}} \,. \tag{9}$$

This function depends only on X_{EIM} and the internal reflection ($k_{1,inner}$ and $k_{1,outer}$). The relationship between X_{EIM} and Q_{EIM} is approximated by a polynomial function:

$$X_{EIM} = \sum_{i=0}^{n_p} p_i \cdot \left(k_2 \cdot Q_{EIM}\right)^i \,. \tag{10}$$

Measurement results and conclusion

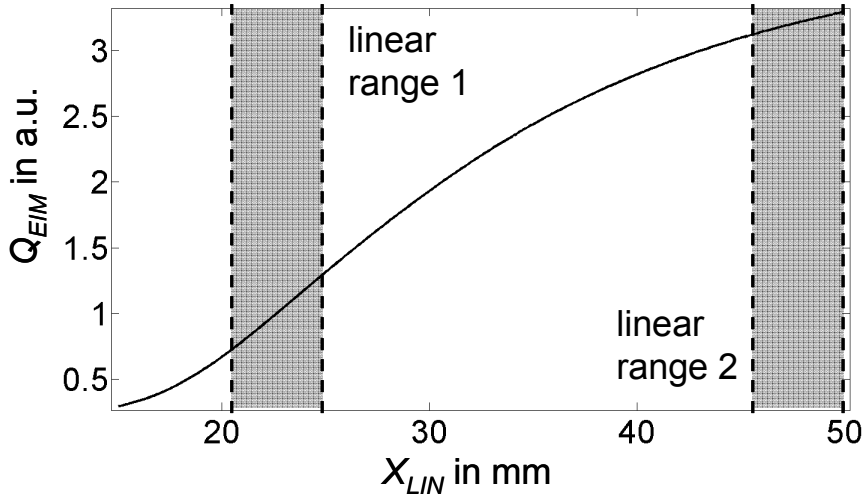

Fig. 2: Measured relationship between X_{LIN} and Q_{EIM}.

The in-process ability of the measurement system during quenching of 900 °C hot rings is qualitatively successfully tested [5]. In order to quantify the modulation function (equation 8), the internal reflection in the sensor glass filter has to be assessed. Here, the illuminated surface is black to maximise the light absorption and has a high roughness (wood) to scatter the reflected light. Additionally, the surface is at least 1 m far away from the sensor. With this setup, the first summand in equation (5) can be neglected, and the recorded values of $U_{PT,outer}$ and $U_{PT,inner}$ are only resulting from the internal reflection.

Figure 2 illustrates the measured relationship between X_{LIN} and Q_{EIM}. In this case, X_{LIN} is the distance between a flat and milled aluminium surface and the front side of the sensor glass filter. It is adjusted by a linear translation stage with a resolution of 0,1 µm. The relationship exhibits two ranges, which can be numerically approximated by a polynomial 1st order according to equation (10). The size of these ranges (4 mm) is chosen by considering the expected movement of a hot ring surface along the sensor measurement direction during quenching in the gas nozzle field. Table 1 shows the characteristics of both linear ranges. S_{EIM} is the measurement sensitivity and results from the product of k_2 and p_1. The standard deviation ΔQ_{EIM} of 100 measuring points at one position X_{LIN} leads to $\Delta X_{EIM,noise}$ according to equation (10) and the Gaussian law of uncertainty propagation. $\Delta X_{EIM,noise}$ is mainly caused by signal noise due to electro-magnetic interferences and represents the lower boundary of the measurement resolution. The ranges 1 and 2 can be approximated but not exactly described by a polynomial 1st order because of principle reasons and possible non-homogeneous surface properties. This fact leads to a non-zero $\Delta X_{EIM,pol1}$, which is calculated by the standard deviation of the differences between the measured and the approximated values of X_{EIM}. It represents a surface dependent measurement resolution of the sensor at a defined and limited range.

Table 1: Characteristics of the sensor at different distances to the measured surface.

	measurement range in mm	S_{EIM} in 1/mm	$\Delta X_{EIM,noise}$ in µm	$\Delta X_{EIM,pol1}$ in µm
linear range 1	21 - 25	0,13	0,3	3
linear range 2	46 - 50	0,04	1	25

The assessment of the sensors reveals two ranges with different characteristics and a linear relationship between the raw data and target data (distance). At linear range 1, the sensors are able to resolve a displacement of 3 µm at a distance between 21 and 25 mm. Hence, they can satisfy the uncertainty requirements of the SFB 570 (< 20 µm) [8]. The spread $\Delta X_{EIM,noise}$ of measured deviations caused by electro-magnetic interferences is negligible.

With the known information about the sensor characteristics, the calibration and evaluation routine for in-process roundness measurements of the steel rings can be developed.

Acknowledgement

The authors thank the German Research Foundation (DFG) for the financial support of the subproject B3 within the Collaborative Research Centre 570 "Distortion Engineering".

References

[1] Dijkman, M.; Ament, C.; Goch, G.: Design and application of quality control strategies at the operational level of a production process chain. Materialwissenschaft und Werkstofftechnik 37 (2009), No. 1, pp.81-84.

[2] Dijkman, M.; Hunkel, M.; Goch, G.: Automatische Qualitätsregelung für die Gasabschreckung von Wälzlagerringen. HTM 62 (2007), No. 4, pp. 173-178.

[3] Dijkman, M.; Goch, G.: Distortion compensation strategies in the production process of bearing rings. Materialwissenschaft und Werkstofftechnik 40 (2009), No. 5-6, pp. 443-447.

[4] Hunkel, M.; Schüttenberg, S.; Frerichs, F.; Fritsching, U.; Mayr, P.: Verzugskompensation mittels Gasabschreckung in flexiblen Düsenfeldern, Teil 2. HTM 59 (2004), No. 5 , pp. 351-357.

[5] Gafsi, H.; Goch, G.: Semi-optical in-process-metrology to determine the roundness deviation of bearing rings during heat treatment. In: Proceedings of IDE 2011, 3rd International Conference on Distortion Engineering. Bremen, Germany, 2011, accepted.

[6] Zhao, Z.; Lau, W. S.; Choi, A. C. K.; Shan, Y. Y.: Modulation functions of the reflective optical fiber sensor for specular and diffuse reflection. Optical Engineering 33 (1994), No. 9, pp. 2986-2991.

[7] Klaiber, J.-A.: Methoden zur Reduzierung der Meßobjekteinflüsse bei der Abstandsmessung mit faseroptischen Streulichtsensoren. Universität Stuttgart, dissertation, 1998.

[8] Stöbener, D.; Dijkman, M.; Kruse, D.; Surm, H.; Keßler, O.; Mayr, P.; Goch, G.: Distance measurements with laser-triangulation in hot environments. In: Metrology in the 3rd Millenium, XVII. IMEKO World Congress, Dubrovnic, Croatia. 2003, pp. 1898-1902.